Diffusion processes in the superionic conductor Li_3N: An NMR study

D. Brinkmann, M. Mali, and J. Roos
Physik-Institut, University of Zurich, Zurich, Switzerland

R. Messer and H. Birli
Max-Planck-Institut für Metallforschung, Institut für Physik, Stuttgart, West Germany
(Received 13 May 1982; revised manuscript received 20 July 1982)

A comprehensive experimental and theoretical NMR study of two diffusion processes in Li_3N is presented: interlayer diffusion parallel to the hexagonal axis involving both Li sites and intralayer diffusion within the Li_2N layers only. The first process allows a quantitative and consistent analysis of the following NMR observables: (i) the second-order quadrupolar shift of the ^7Li central signal and its strong temperature dependence between 400 and 600 K, and (ii) the temperature dependence (above 420 K) and the extreme angle dependence of the ^7Li and ^6Li relaxation rates by taking into account different relaxation mechanisms for both isotopes. The activation energy (0.62 eV) and the correlation times agree with values deduced from conductivity measurements. The intralayer diffusion process is studied by means of the temperature and angle dependence of ^6Li and ^7Li relaxation times below 320 K. The Li(2) vacancy concentration is determined in agreement with x-ray data.

I. INTRODUCTION

The ionic conductor lithium nitride Li_3N has recently attracted considerable theoretical and technological interest. The latter arises mainly from its high Li-ion conductivity of about 10^{-3} $(\Omega\,\mathrm{cm})^{-1}$ at room temperature, its simple preparation, and its stability with elemental Li which shows Li_3N to be one of the best candidates for an electrolyte in a lithium-based solid-state battery.[1]

On the other hand, because of its relatively simple structure, Li_3N serves as a model substance for studying fundamental questions about superionic conductors. For a review of the numerous investigations performed in Li_3N see Ref. 2. The crystal structure is illustrated in Fig. 1. Li_3N crystallizes in space group $P6/mmm$. The N atom is coordinated by six Li(2) atoms in a hexagonal Li_2N plane plus a Li(1) atom occupying a central site in the elementary cell on each side above and below the Li_2N plane. Therefore, Li_3N can also be considered as a layer structure with alternately Li_2N layers and pure Li layers perpendicular to the c axis.

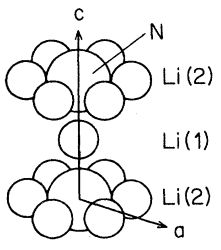

FIG. 1. Crystal structure of Li_3N. $c=3.875$ Å, $a=3.648$ Å.

Nuclear magnetic resonance (NMR) investigations have played an active role in the study of Li_3N. Earlier NMR work[3–5] was mainly concerned with the question of whether the chemical bonding is of ionic or covalent character. More recent studies[6–14] employing high-quality single crystals are strongly devoted to elucidate the diffusion mechanisms in Li_3N although some modern work[15] has again studied the ionic nature of bonding.

Li NMR offers some particular advantages since Li nuclei consist of two magnetic isotopes, ^6Li and ^7Li, differing in their nuclear properties. ^7Li nuclei with a natural abundance of 92.57 at.% have a much larger electric quadrupole moment than ^6Li nuclei (7.43 at.% abundance), the ratio being given by $Q(^6Li)/Q(^7Li)=0.019$. On the other hand, the corresponding ratio of the magnetic dipole moments is 0.2524. Thus, studying both resonances allows a double check of models which have been evoked to describe diffusion phenomena and provides detailed information on the electric and magnetic interaction of the Li nuclei.

In this paper we present a comprehensive account on experimental and theoretical NMR studies of two diffusion processes in Li_3N: intralayer diffusion involving Li(2) ions only and interlayer diffusion involving both Li(1) and Li(2) ions. The presence of

these diffusion processes has been deduced from a large body of experimental data taken between 210 and 670 K and concerning three observables: (i) the second-order quadrupolar shift of the ^{7}Li signal, (ii) the various relaxation rates of ^{7}Li and their angle dependence, and (iii) the relaxation rates of ^{6}Li. The results for a fourth observable, the ^{7}Li linewidth, discussed previously[11] are in agreement with the conclusions presented here.

With the use of a simple model to describe the interlayer diffusion process, the data are handled in a consistent theoretical treatment yielding the *same* temperature-dependent correlation time for all three sets of experimental data. This result unambiguously proves that Li diffusion along the c axis, which is responsible for the extremely anisotropic conductivity, involves both Li sites in contrast to x-ray studies[16] which postulate an exchange of Li(2) atoms belonging to different layers without involving Li(1) atoms.

The intralayer diffusion process is described by a two-dimensional isotropic diffusion model. As a result, one obtains the vacancy probability for the Li(2) ions.

This paper is organized as follows. In Sec. II we describe details about the experimental procedures and present the results. The theoretical calculation of the frequency shift and of relaxation times arising from the interlayer process is sketched in Sec. III and is given in detail in the Appendix. The intralayer process is dealt with in Sec. IV. Finally, in Sec. V we discuss the experimental results with respect to theory.

II. EXPERIMENTAL DETAILS AND RESULTS

As in our previous studies[6–13] Czochralski-grown single crystals[17] were used which we obtained from the Max-Planck-Institut für Festköperforschung, Stuttgart. Experiments were performed with specimens belonging to different crystal batches. In contrast to the linewidth data,[11] only undoped samples were investigated and no significant sample dependence of the data could be detected.

The ^{6}Li- and ^{7}Li-NMR signals were observed with pulse spectrometers at frequencies ranging from 8 to 35 MHz. The signals were digitized by transient recorders and accumulated and Fourier transformed by on-line computers. Line positions were determined from the Fourier transform of the free-induction decay signal following a $\frac{1}{2}\pi$ radio-frequency pulse. To measure relaxation times the saturation method was employed: A sequence of several $\frac{1}{2}\pi$ pulses is applied to the sample in order to totally saturate the NMR line. The subsequent recovery of the signal is measured by means of a $\frac{1}{2}\pi$ pulse. At high temperatures where T_1 becomes comparable to T_2, relaxation times were measured by the $\pi-(\pi/2)$ pulse sequence. Probe temperatures were monitored within ± 1 K by means of thermocouples or platinum resistors.

Owing to electric quadrupole interaction, the spin-$\frac{3}{2}$ ^{7}Li spectrum arising from Li(1) and Li(2) sites, respectively, consists of one central and two satellite lines. Since the quadrupole interaction is small with respect to the Zeeman interaction, the two central lines, being shifted only in second order, strongly overlap. The ^{6}Li spectrum (spin 1) consists of one doublet for each Li site. At room temperature the ^{7}Li quadrupole coupling constants which we have determined previously[6,15] are $eQV_{z'z'}/h = 582 \pm 3$ kHz for Li(1) and 284 ± 1 kHz for Li(2), where $V_{z'z'}$ is the principal component of the electric field gradient (EFG) tensor along the symmetry axis which is parallel to the c axis. The corresponding values for ^{6}Li are 11.7 and 5.7 kHz, respectively.[7]

As described previously,[6,9] raising the temperature causes the two ^{7}Li central lines to merge completely into a single line, while the satellite lines of both sites become less intense, broaden, and eventually disappear. Above 450 K the satellites recover again; however, the corresponding coupling constant is drastically reduced. We have attributed these facts to the aforementioned interlayer diffusion process by which Li ions jump from a site (1) to a site (2) and vice versa, thus averaging the EFG "seen" by the Li nuclei.

In our present work we have measured in the whole temperature range between 380 and 670 K the second-order shift of the "averaged" ^{7}Li central signal for several values of θ, the angle between the c axis and the magnetic field. The results are plotted in Fig. 2 for $\theta = 42°$ and 90° for which angles the shifts exhibit extreme values with respect to the Larmor frequency. From 380 to 450 K the shifts are constant, then start to decrease and become negligibly small above 600 K. The solid curves in Fig. 2. as well as in the following figures are theoretical predictions to be discussed in Sec. IV.

We turn now to the results of the relaxation time measurements. As found in our earlier work[6] the relaxation of the ^{7}Li central signal is governed in general by two relaxation rates R_1 and R_2, except for some special angles θ. If the central line is sa-

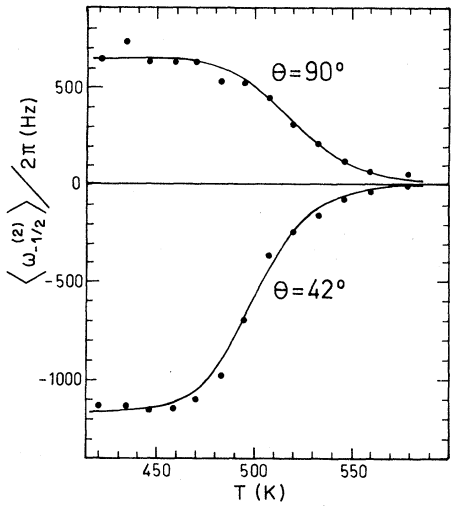

FIG. 2. Temperature dependence of the quadrupolar second-order shift of the "averaged" ^{7}Li central signal for $\theta=42°$ and 90°. θ is the angle between the c axis and the magnetic field. (Larmor frequency $\nu_L=12.0$ MHz.)

turated the recovery of the signal height $S(t)$ may be described by

$$S(t)=S_0+S_1\exp(-R_1t)+S_2\exp(-R_2t) \tag{1}$$

with

$$S_1=S_2=-\frac{S_0}{2}\ .$$

For reasons to be explained later, the temperature dependence of the ^{7}Li relaxation rates has been determined for various values of the angle θ. Most of the data have been taken at $\theta=0°$, 90°, and 25°. The results for $\theta=0°$ and 90° are plotted in Fig. 3 over the whole temperature range investigated. Two different regions are clearly distinguished: The high-temperature relaxation rates are attributed to the interlayer process while the low-temperature relaxation values are due to the intralayer process. According to the model calculations for the interlayer process to be discussed in Secs. III and V, only one nonzero rate should be observed at $\theta=90°$. However, due to a slight misalignment of the crystal, a second rate is obtained which is more than ten times smaller than the first rate. In Fig. 3, for sake of clarity, this smaller rate is presented only for the measurements at 34.5 MHz. To get a better resolution of the data at the high-temperature maxima, they are plotted separately in Figs. 4 and 5 for $\theta=90°$ and 25°, respectively. The angle dependence of the ^{7}Li relaxation is given in Fig. 6 for two elevated temperatures and in Fig. 7 for room temperature.

The relaxation rates of ^{6}Li have been measured as a function of temperature at $\theta=0°$ and $\theta=90°$ (Fig. 8). The angle dependence of the ^{6}Li relaxation is given for three different temperatures (Fig. 9).

III. INTERLAYER DIFFUSION

In this section we sketch the calculation in the high-field limit of the spin-lattice relaxation times

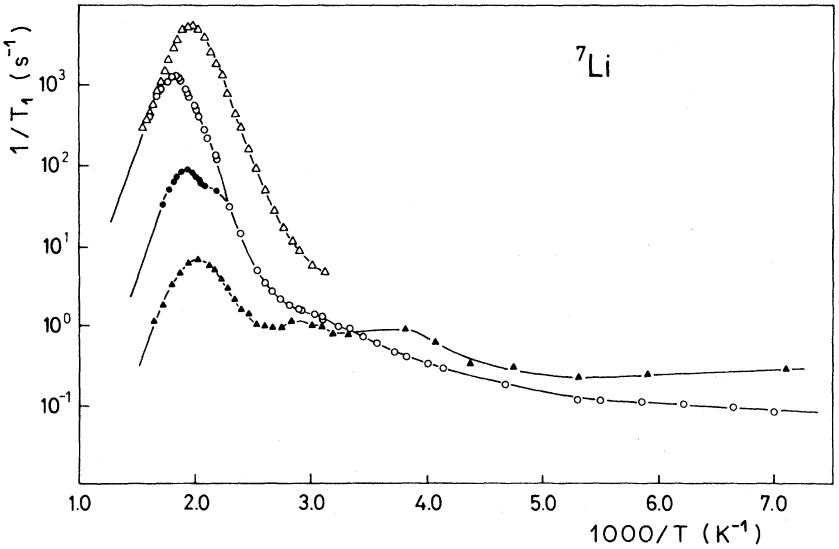

FIG. 3. Spin-lattice relaxation rate of ^{7}Li as a function of inverse temperature for two orientations and two Larmor frequencies. $\theta=90°$: (△) 8 MHz; (○,●) 34.5 MHz. $\theta=0°$: (▲) 34.5 MHz. The lines are drawn to guide the eye.

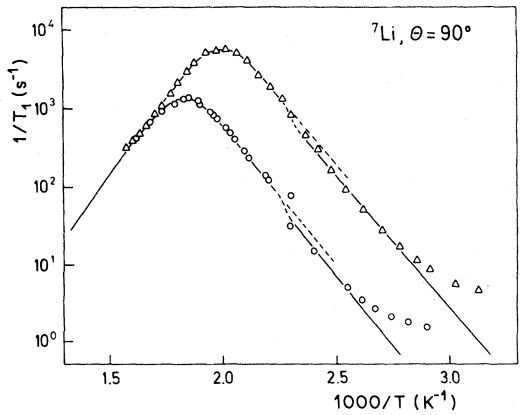

FIG. 4. Spin-lattice relaxation rates of ^{7}Li vs inverse temperature for $\theta = 90°$ and two Larmor frequencies: (△) 8 MHz and (○) 34.5 MHz. The lines represent the fitted theoretical expressions for the interlayer process.

for ^{6}Li and ^{7}Li and the second-order quadrupolar shift of the ^{7}Li central signal by assuming the interlayer diffusion process to be the dominant mechanism.

The basic assumption is the following: Li ions of site (1) and (2) may exchange places via some interstitial positions. However, we assume that the time spent at these interstitial positions is negligible compared with the mean residence time at the regular positions. Therefore, the time-dependent component $V_{ij}(t)$ of the tensor "seen" by a jumping Li ion may be written as

$$V_{ij}(t) = P^{(1)}(t)V_{ij}^{(1)} + P^{(2)}(t)V_{ij}^{(2)} , \qquad (2)$$

where $V_{ij}^{(1)}$ and $V_{ij}^{(2)}$ are the V_{ij} components at the

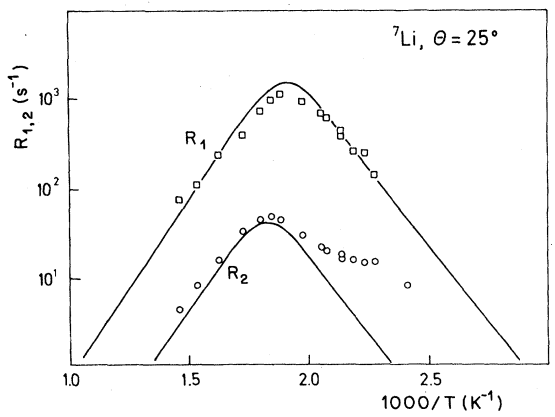

FIG. 5. Spin-lattice relaxation rates of ^{7}Li vs inverse temperature for $\theta = 25°$ and Larmor frequency 35 MHz. The lines represent the fitted theoretical expressions for the interlayer process.

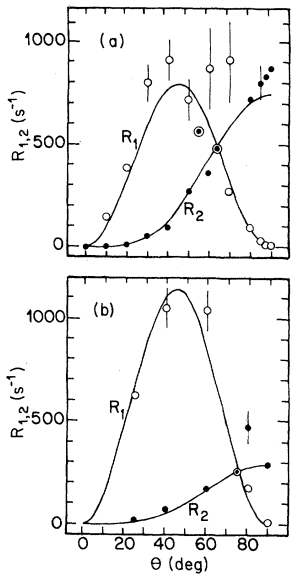

FIG. 6. Angle dependence of ^{7}Li-spin-lattice relaxation rates at two elevated temperatures: (a) $T = 593$ K, $\omega = 2\pi(9.2 \times 10^6\ s^{-1})$, $\omega\tau < 1$. (b) $T = 483$ K, $\omega = 2\pi(3.5 \times 10^7\ s^{-1})$, $\omega\tau > 1$. The lines represent the fitted theoretical expressions for the interlayer process.

atomic sites (1) and (2), respectively, and $P^{(1)}$ and $P^{(2)}$ are occupation probabilities defined by $P^{(k)} = 1$ if the ion occupies site k, and $P^{(k)} = 0$ otherwise. Since there are twice as many Li(2) positions as Li(1) positions the ensemble averages of the $P^{(k)}$ are $\langle P^{(1)} \rangle = \frac{1}{3}$ and $\langle P^{(2)} \rangle = \frac{2}{3}$ if all sites are fully occupied.

The fluctuating EFG's cause both spin-lattice relaxation and a temperature-dependent second-order quadrupolar shift of the central line. We now proceed to calculate these effects.

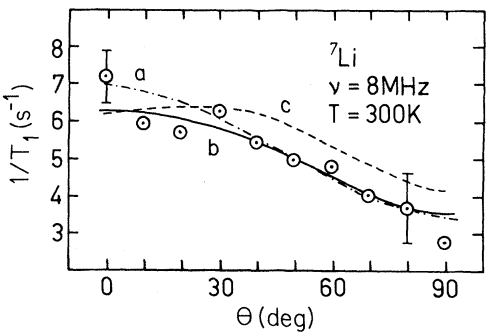

FIG. 7. Angle dependence of ^{7}Li-spin-lattice relaxation rate at 300 K. The curves correspond to a fit of Eq. (12) for various values of $\omega\tau_Q$. (a) $\omega\tau_Q \ll 1$; (b) $\omega\tau_Q = 0.5$; (c) $\omega\tau_Q = 1$.

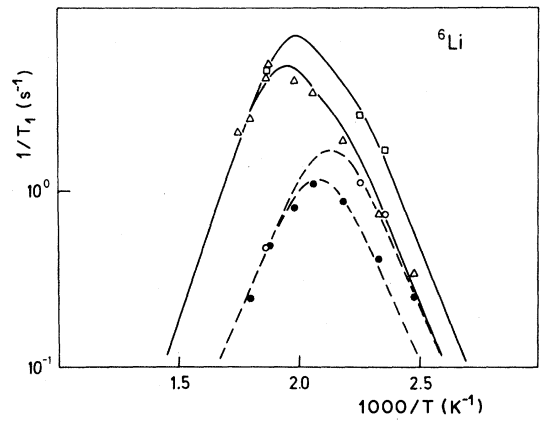

FIG. 8. ^{6}Li-spin-lattice relaxation rate vs inverse temperature for two orientations and two Larmor frequencies. $\theta=90°$: (△) 13.2 MHz, (□) 9.1 MHz. $\theta=0°$: (●) 13.2 MHz, (○) 9.1 MHz. The fits to theoretical expressions for the interlayer process are represented by full lines (90°) and broken lines (0°).

A. Spin-lattice relaxation

We assume a well-resolved quadrupole spectrum so that spin-exchange transitions are suppressed. The influence of the so-called lattice-induced spin exchange transitions[11] can be neglected within the framework of this treatment. Then, the spin-lattice relaxation of the nuclei is in general described by $2I$ relaxation rates. The initial conditions being such that the transverse magnetization is zero, the relaxation rates may be calculated in a conventional manner from the rate equations determining the difference in population between adjacent nuclear levels.[18]

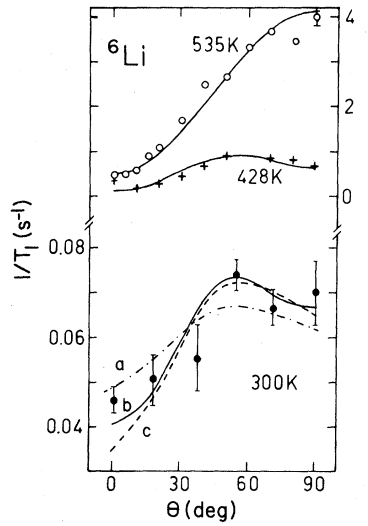

FIG. 9. Angle dependence of ^{6}Li-spin-lattice relaxation rate for three temperatures at a Larmor frequency of 13.2 MHz. The lines correspond to fitted theoretical expressions for the interlayer process (535, 428 K) and for the intralayer process (300 K). The 300-K data are fitted with different values for $\omega_I\tau_D$. (a) $\omega_I\tau_D=0.5$. (b) $\omega_I\tau_D=0.8$. (c) $\omega_I\tau_D=1$.

If the populations of the levels are N_m, and the difference in population $N_{m+1}-N_m$ between adjacent levels is called $N_{m+1/2}\equiv N_p$, the general solution of the rate equations for $I=\frac{3}{2}$ is of the form

$$N_p=n_0+\sum_{\substack{q=1\\p=0,\pm1}}^{3} a_{pq}\exp(-R_q t)\,, \tag{3}$$

where n_0 is the equilibrium value of N_p and the coefficients a_{pq} are determined by the initial conditions. For the relaxation rates R_q we obtain the three values

$$\begin{aligned} R_1&=W_1+W_2+7W\\ &\quad+[(W_1-W_2+3W)^2+16W^2]^{1/2}\,,\\ R_2&=W_1+W_2+7W\\ &\quad-[(W_1-W_2+3W)^2+16W^2]^{1/2}\,,\\ R_3&=2(W_1+W_2)+6W\,. \end{aligned} \tag{4}$$

For $I=1$, the relaxation is governed by a single relaxation rate:

$$R=W_1+4W_2+2W\,. \tag{5}$$

The quantities W_1, W_2, and W, being independent of the magnetic quantum number m, are a measure of the transition probabilities: W_1 and W_2 for the transitions $\Delta m=1$ and $\Delta m=2$, respectively, induced by quadrupole interaction, and W for the $\Delta m=1$ transition due to magnetic interaction. These quantities depend on the detailed form of the various relaxation mechanisms and they are functions of temperature and crystal orientation.

The calculation of W_1 and W_2 is given in Appendix A. Assuming an exponential decay of the EFG correlation function with correlation time τ, we obtain

$$W_1=\frac{3\pi^2}{4I}(C_1^2+2C_2^2)\sin^2\theta\cos^2\theta\frac{\tau}{1+\omega^2\tau^2}\,, \tag{6}$$

$$W_2=\frac{3\pi^2}{16I}(C_1^2+2C_2^2)\sin^4\theta\frac{\tau}{1+4\omega^2\tau^2}\,. \tag{7}$$

Here θ is the angle between the external magnetic field and the hexagonal axis which is parallel to the

EFG symmetry axis at the Li sites. C_1 and C_2 are the quadrupole coupling constants defined by Eq. (A7) for the Li sites (1) and (2), respectively. This treatment of quadrupole relaxation is based on the assumption that spin-exchange effects may be neglected. However, if the spacing of the NMR lines becomes comparable to the dipolar linewidth, a common temperature of the spin system is established by rapid spin-spin interactions and a single relaxation rate given by[18]

$$\frac{1}{T_1}=\frac{2I+3}{5I(2I-1)}(W_1+4W_2) \tag{8}$$

will be observed.

The transition probability W is related to the Fourier transform of a fluctuating magnetic field. If we consider a nuclear spin system I (for instance, the ^{6}Li system) coupled by dipole-dipole interaction to another spin system S (the ^{7}Li system) which has a relaxation mechanism of its own being much stronger than that due to its coupling with the nuclear spin system I, W is given by[19]

$$W=\frac{3\pi}{2}\gamma_I^2\gamma_S^2\hbar^2S(S+1)\times[\tfrac{1}{18}J_0(\omega_I-\omega_S)+J_1(\omega_I)+\tfrac{1}{2}J_2(\omega_I+\omega_S)], \tag{9}$$

where the γ's and ω's are the magnetogyric ratios and frequencies of the I and S system, respectively, and J_0, J_1, and J_2 are the spectral densities of the correlation function of the fluctuating dipole coupling.

B. Second-order quadrupolar shift

To calculate the temperature-dependent second-order quadrupolar shift of the ^{7}Li central signal we start with an expression derived independently by Bjorkstam and Villa,[20] using a general time-dependent formalism to treat second-order effects upon line shape, and by Schimmele.[21] Again an exponential decay of the EFG correlation function with correlation time τ is assumed. Then, as shown in Appendix B the second-order frequency shift of the central signal of a spin-$\frac{3}{2}$ quadrupolar splitting is given by

$$\langle\omega^{(2)}_{-1/2}\rangle=-\frac{\pi^2}{6\omega}\left[\sin^2\theta\cos^2\theta(C_1+2C_2)^2\frac{1}{1+\omega^2\tau^2}+3\sin^2\theta\cos^2\theta(C_1^2+2C_2^2)\frac{\omega^2\tau^2}{1+\omega^2\tau^2}\right.$$
$$\left.-\tfrac{1}{8}\sin^4\theta(C_1+2C_2)^2\frac{1}{1+4\omega^2\tau^2}-\tfrac{3}{8}\sin^4\theta(C_1^2+2C_2^2)\frac{4\omega^2\tau^2}{1+4\omega^2\tau^2}\right]. \tag{10}$$

τ, ω, θ, C_1, and C_2 have the same meaning as in Eqs. (6) and (7).

Note that the quadrupole coupling constants C_1 and C_2 appear in two ways: as a sum squared and as a sum of coupling constants squared. Thus, in contrast to the transition probabilities W_1 and W_2 [Eqs. (6) and (7)], the second-order shift is sensitive to the relative sign of the coupling constants which will become essential in interpreting the experimental data.

IV. INTRALAYER DIFFUSION

In this section we calculate the spin-lattice relaxation times for ^{6}Li and ^{7}Li arising from an isotropic diffusion of Li(2) vacancies in the Li_2N layers. The presence of these vacancies with a concentration of the order of 1% has been suggested by an interpretation of x-ray data.[16] The vacancies are treated as point charges with charge e diffusing independently and isotropically in the Li_2N layers thus producing fluctuating EFG's and magnetic fields at a stationary Li(2) nucleus. This treatment is similar to the three-dimensional example given by Cohen and Reif.[22]

We assume that the ^{7}Li spins, due to their large quadrupole moment, are relaxed by electric interactions only. Hence, the transition probabilities W_1 and W_2 are again given by Eqs. (A1) and (A2). Taking into account contributions only from those vacancies diffusing in the same layer which contains the stationary nucleus, we find the averaged field gradient components defined in Eqs. (A3):

$$\langle |V_1|^2\rangle=(\pi/4)nd^{-4}(3e\beta)^2(\sin^2\theta-\tfrac{3}{4}\sin^4\theta)\,,$$
$$\langle |V_2|^2\rangle=(\pi/2)nd^{-4}(\tfrac{3}{2})^2(e\beta)^2(\cos^2\theta+\tfrac{3}{8}\sin^4\theta)\,. \tag{11}$$

Here n is the density of moving vacancies within the particular layer considered, d is the distance of closest approach of a vacancy to the nucleus, and θ denotes the angle between the magnetic field and the crystallographic c axis. The factor β takes into account antishielding and polarization effects.[22] Substitution of Eq. (11) in (A1) and (A2) yields

$$W_1=\frac{3}{16}\left[\frac{e^2\beta Q}{\hbar}\right]^2 d^{-4}\frac{n\tau_Q}{1+\omega^2\tau_Q^2}(\sin^2\theta-\tfrac{3}{4}\sin^4\theta)\,,$$
$$W_2=\frac{3}{32}\left[\frac{e^2\beta Q}{\hbar}\right]^2 d^{-4}\frac{n\tau_Q}{1+4\omega^2\tau_Q^2}(\cos^2\theta+\tfrac{3}{8}\sin^4\theta),$$

where τ_Q is the correlation time of the fluctuating EFG. If a common spin temperature exists the relaxation rate is given by Eq. (8), and we obtain for the ^{7}Li spin system

$$\frac{1}{T_{1\perp}(7)}=\frac{3}{40}\left[\frac{e^2\beta Q}{\hbar}\right]^2 d^{-4}n\left[(\sin^2\theta-\tfrac{3}{4}\sin^4\theta)\frac{\tau_Q}{1+\omega^2\tau_Q^2}+2(\cos^2\theta+\tfrac{3}{8}\sin^4\theta)\frac{\tau_Q}{1+4\omega^2\tau_Q^2}\right]. \tag{12}$$

The symbol $\perp$ refers to the Li_2N layers perpendicular to the c axis.

We now turn our attention to the ^{6}Li relaxation. Here, in contrast to the ^{7}Li relaxation, we assume the magnetic interaction to be the dominant relaxation mechanism since the ^{6}Li quadrupole moment is so small. Hence, Eq. (9) is applicable, where I denotes the ^{6}Li system, and S the spin of the ^{7}Li nuclei. Expressions for the spectral densities J_0, J_1, and J_2 may be found in Ref. 19 and may be evaluated in a way similar to the calculation of the V_i of Eq. (11). The final result is

$$\frac{1}{T_{1\perp}(6)}=\frac{\pi}{2}\gamma_I^2\gamma_S^2\hbar^2S(S+1)d^{-4}n\left[\tfrac{1}{6}(1-3\sin^2\theta)\frac{\tau_D}{1+(\omega_I-\omega_S)^2\tau_D^2}+\tfrac{2}{3}(\sin^2\theta-\tfrac{3}{4}\sin^4\theta)\frac{\tau_D}{1+\omega_I^2\tau_D^2}\right.$$
$$\left.+\tfrac{2}{3}(\cos^2\theta+\tfrac{3}{8}\sin^4\theta)\frac{\tau_D}{1+(\omega_I-\omega_S)^2\tau_D^2}\right], \tag{13}$$

where τ_D denotes the correlation time of the magnetic fluctuations. In Table I are summarized the various correlation rates used in this and in the following sections.

V. DISCUSSION

In this section we are going to show how the experimental data can be explained in terms of the inter- and intralayer diffusion processes. We will discuss the frequency shifts and relaxation rates separately.

A. Interlayer diffusion

1. *Second-order quadrupolar shift of ^{7}Li*

It was the temperature dependence of this shift which gave the first clue to the interlayer process.[6]

Examination of Eq. (10) reveals that with respect to the correlation time τ two regimes may be distinguished: (i) The slow motion regime, i.e., $\omega\tau\gg1$, where the terms involving $C_1^2+2C_2^2$ are dominating and the shift is nearly independent of τ. This case is obviously met at lower temperatures between 400 and 450 K. (ii) The fast motion regime ($\omega\tau\ll1$) at higher temperatures when the terms involving $(C_1+2C_2)^2$ are large compared to the others. However, in this regime the resulting shift is small, as observed experimentally, only if C_1 and C_2 have opposite signs, which was confirmed theoretically.[15] Thus, in the limiting cases $\omega\tau\gg1$ and $\omega\tau\ll1$, Eq. (10) reduces to the well-known expression[19]

$$\langle\omega^{(2)}_{-1/2}\rangle=\frac{3\pi^2}{16\omega}C_{\rm eff}^2(1-\cos^2\theta)(1-9\cos^2\theta)$$

for the second-order shift with an effective coupling constant $C_{\rm eff}=(\frac{1}{3}C_1^2+\frac{2}{3}C_2^2)^{1/2}$ in the limit $\omega\tau\gg1$ and $C_{\rm eff}=\frac{1}{3}C_1+\frac{2}{3}C_2$ in the limit $\omega\tau\ll1$.

Having established a qualitative agreement be-

TABLE I. Various correlation rates used in the text.

Symbol	Definition	Inferred from
$1/\tau$	Correlation rate of fluctuating electric and magnetic fields due to interlayer diffusion (identified with jump rate of Li atoms)	Second-order quadrupolar shift of ^{7}Li and T_1 of ^{7}Li and ^{6}Li
$1/\tau_v$	Hopping rate of Li(2) vacancies	
$1/\tau_{v0}$	Prefactor of $1/\tau_v$	Temperature dependence of T_1 of ^{7}Li
$1/\tau_Q$	Correlation rate of fluctuating electric field gradient due to intralayer diffusion [identified with hopping rate of Li(2) vacancies]	Angle dependence of T_1 of ^{7}Li at 300 K ($\tau_Q \leq 2\times10^{-8}$ s)
$1/\tau_D$	Correlation rate of fluctuating magnetic fields due to intralayer diffusion	Angle dependence of T_1 of ^{6}Li at 300 K ($\tau_D \approx 10^{-8}$ s)
$1/\bar{\tau}$	Mean jump rate of Li(2) atoms in the intralayer diffusion	Motionally narrowed linewidth[a] (10^{-7} s $\leq \bar{\tau} \leq 10^{-6}$ s)

[a]Reference 11.

tween the experimental data and Eq. (10), we may calculate the correlation time τ by inserting the experimental values of the shift into Eq. (10). In Fig. 10, $1/\tau$ is plotted versus inverse temperature, showing that $1/\tau$ follows an Arrhenius law $1/\tau = 1/\tau_0 \exp(-E/kT)$, where E is an activation energy. Furthermore, the correlation time does not depend on the NMR frequency. A least-squares fit yields

$$E = (0.68 \pm 0.08)\ ,$$

$$1/\tau_0 = (7 \pm 4) \times 10^{14}\ ,$$

with E in units of eV, and $1/\tau_0$ in units of s^{-1}. We will discuss these results after dealing with the relaxation data.

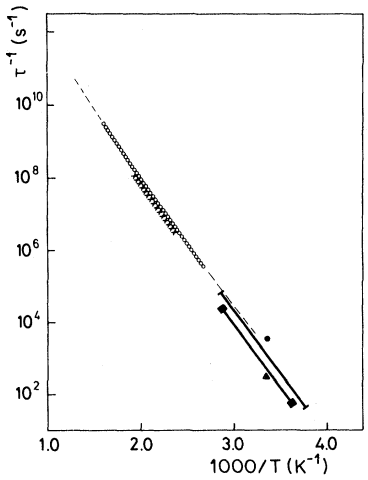

FIG. 10. Temperature dependence of correlation rate τ^{-1} for the interlayer process obtained from NMR and from conductivity data parallel to the c axis. (ooo), τ^{-1} calculated from spin-lattice relaxation data; ($\times\times\times$), τ^{-1} calculated from quadrupolar second-order shift; (|—|,■—■), τ^{-1} values from conductivity data of Ref. 24; (●,▲), τ^{-1} values from conductivity data of Ref. 25.

2. *Relaxation of ^{7}Li*

Besides causing the temperature-dependent quadrupolar shift, the interlayer diffusion also establishes a powerful relaxation mechanism since the jumping Li nuclei experience a fluctuating EFG not

only changing its magnitude but also its sign. In Figs. 4 and 5, the relaxation rates at temperatures above 420 K show the typical Bloembergen-Purcell-Pound (BPP)-type behavior which is predicted by Eqs. (6) and (7) for a thermally activated correlation time τ. Taking into account the results of the shift measurements, we assume that the ^{7}Li relaxation in this temperature range is almost exclusively determined by the interlayer process via quadrupolar interaction.

According to Eq. (4), in general three relaxation rates are expected. Since the ^{7}Li spectrum is excited symmetrically by the radio-frequency pulses the initial conditions for the differences in populations N_p are symmetric, and Eq. (3) allows for two solutions only in agreement with the experimental results. These rates, R_1 and R_2, have prefactors a_{01} and a_{02} of equal magnitude in accord with the experimental result described by Eq. (1). These rates are determined only by the quadrupole transition probabilities W_1 and W_2, since the magnetic probability W is negligibly small.

First, we examine the angle dependence of the ^{7}Li relaxation rates at 483 and 593 K (see Fig. 6) to prove our assumption that the interlayer diffusion process is the dominant relaxation mechanism. The experimental data may be fitted by Eqs. (6) and (7) with $\omega\tau$ as the only adjustable parameter. $\omega\tau=5$ and $\omega\tau=0.15$, respectively, give reasonable agreement between theory and experiment for both rates. Of course, at $\theta=0°$ where $W_1=W_2=0$, and at $\theta=90°$, where $W_1=0$, some other relaxation mechanisms must be responsible for the finite rates measured, as for instance quadrupolar relaxation due to mechanisms different from the interlayer diffusion process or magnetic relaxation. The "crossing point," where W_1 and W_2 become equal, will be discussed later.

Next, we examine the temperature dependence of the ^{7}Li relaxation rate at about 500 K. The angle dependence has shown that at $\theta=90°$ the quadrupolar relaxation rate R_2 due to interlayer diffusion is rather high. Especially, at the maximum, R_2 is at least 2 orders of magnitude higher than relaxation rates caused by other processes, e.g., magnetic interactions. Therefore, we only keep R_2 for the following analysis.

The shape of the relaxation rate curve around its maximum points to the fact that the correlation time τ does not obey a simple Arrhenius law. The precision of the ^{7}Li relaxation data allows a more refined interpretation than was possible with the quadrupolar shift data. Since the EFG at a Li site changes only when the Li atom jumps to a nonequivalent site, we identify the correlation rate $1/\tau$ with the jump rate of the Li atoms in the interlayer diffusion. This rate depends on the number of Li(1) and Li(2) vacancies. From x-ray studies it has been concluded[16] that the Li(1) sites are fully occupied, while the Li(2) sites have an underoccupancy of about 1% at room temperature, which increases with rising temperature. However, since the interlayer diffusion means that Li(1) and Li(2) atoms exchange places a small concentration on Li(1) vacancies not detectable by x-rays must be assumed. If c is the fractional number of Li(1) and Li(2) vacancies, the hopping rate of Li atoms may be written as

$$\frac{1}{\tau}=c\frac{1}{\tau_v}\ , \tag{14}$$

where $1/\tau_v$ is the hopping rate for a vacancy to hop between sites (1) and (2). Because of its temperature dependence, we decompose c into two terms, c_0 and $c(T)$, where c_0 stands for the temperature-independent and $c(T)$ for the thermally activated part of the vacancy concentration. One therefore has

$$c=c_0+c(T)=c_0+c_0'\exp(-E^F/kT)\ ,$$

where c_0' is an appropriate prefactor and E^F the formation enthalpy of a vacancy. For a Frenkel defect, c_0' is given by

$$c_0'=\exp(\Delta S^F/k)\ ,$$

where ΔS^F is the entropy of formation.

We assume the hopping rate of a vacancy, $1/\tau_v$, to be thermally activated, i.e.,

$$1/\tau_v=(1/\tau_{v0})\exp(-E^M/kT)\ .$$

Here E^M is the barrier height for vacancy migration and $1/\tau_{v0}$ is the "attempt" frequency. We thus obtain for the hopping rate of Li ions

$$1/\tau=(1/\tau_{v0})\exp(-E^M/kT)\times[c_0+c_0'\exp(-E^F/kT)]\ . \tag{15}$$

By inserting this expression into Eq. (7) the temperature dependence of the relaxation rates has been fitted.

Figure 4 shows that the agreement between the experimental data and the theoretical curves is rather good. The fitted parameters are

$$E^M = 0.62 \pm 0.3 \text{ ,}$$
$$\frac{\tau_{v0}}{c_0} = 9.5 \times 10^{-15} \text{ ,}$$
$$E^F = 0.2 \pm 0.05 \text{ ,} \tag{16}$$
$$\frac{c_0'}{c_0} = 120 \text{ ,}$$

with E^M and E^F in units of eV, and τ_{v0}/c_0 in s.

It must be noted that the parameters could not be determined completely independently from one another. Increasing the activation enthalpy E^M of the jump process leads to a decrease of the formation enthalpy E^F without changing the mean standard deviation considerably. Therefore, the errors given are much higher than determined from the fitting procedure.

Since the fit parameters do not yield the absolute values of c_0 and c_0' we can only qualitatively compare our result with the x-ray data. Taking from Ref. 16 the value $c_0 = 0.01$, the temperature dependence of the vacancy concentration as determined by x-rays[16] is well accounted for by our parameters c_0' and E^F.

If we adopt $c_0 = 0.01$ the prefactor $1/\tau_{v0}$ would be about 10^{16} Hz, which is too high for an optical phonon frequency. However, $1/\tau_{v0}$ may be split into two factors, one representing a real "attempt" frequency, the second—similar to c_0'—may be written as $\exp(\Delta S^M/k)$, where ΔS^M is the entropy of migration.[23] The high entropy reflects the large number of sites a given vacancy may hop to: regular and interstitial sites within the Li_2N layer and in neighboring layers of both types, Li_2N and pure Li layers. On the low-temperature side of the relaxation rate maximum, the transition of the spin system to a common spin temperature can clearly be seen. The jump of the rate corresponds exactly to the change of $R_2 = 2W_2$ given by Eq. (7) to the new value $1/T_1$ as given by Eq. (8).

The results for the relaxation rate of ^{7}Li at $\theta = 25°$, shown in Fig. 5, are nearly identical to those obtained at $\theta = 90°$. The theoretical curves are plotted with the parameters mentioned above to fit the data at $\theta = 90°$ and with the help of Eqs. (4), (6), and (7). No additional parameter was used. The slight discrepancy between experimental data and theoretical curves could be removed by taking into account an error of about 1° for the angle θ and an additional weak contribution from dipolar interactions as suggested by the ^{6}Li data to be discussed later. The deviation at the low-temperature side of the smaller relaxation rate R_2 can be related to the so-called lattice-induced spin exchange relaxation discussed elsewhere.[12] The measurements at $\theta = 0°$ will not be discussed here. At this angle the quadrupolar relaxation of the interlayer diffusion should be zero [Eqs. (6) and (7)]. Because of a slight misalignment of the crystallographic c axis with the magnetic field, the quadrupolar contributions W_1 and W_2 become comparable with the contributions from magnetic interactions and the interpretation of the data is rather difficult and tedious.

Finally, we comment on the "crossing point," i.e., the angle θ^* where W_1 and W_2 become equal. According to Eq. (A10), θ^* is shifted to lower values for decreasing correlation time τ. Table II lists the range of angles where only a single relaxation rate could be detected. The corresponding theoretical values have been calculated with the help of Eqs. (A10), (15), and (16). The agreement with the experimentally determined values of θ^* provides an additional support of our model for the interlayer diffusion. Of course, a single relaxation rate is also observed at the "magic angle" $\theta = 54.7°$. There the quadrupole splitting vanishes and a common spin temperature is established leading to a single rate $1/T_1$ given by Eq.(8).

3. *Relaxation of ^{6}Li*

For ^{6}Li with spin 1, the relaxation is governed by a single relaxation rate [see Eq. (5)]. Since ^{6}Li has a very small quadrupole moment, one is tempted to assume that quadrupolar relaxation of ^{6}Li is negligibly small and that the observed relaxation rates

TABLE II. Temperature dependence of the "crossing point" angle θ^* (Larmor frequency 35 MHz).

Temperature T (K)	Correlation time τ (s)	θ^* (deg) Theoretical	Experimental
483	1.4×10^{-8}	76	74–78
542	2.1×10^{-9}	68	67–73
604	3.9×10^{-10}	64	53–66

are due to magnetic interaction.[7] However, we will show in this section that the ^{6}Li relaxation rates are due to both quadrupolar and magnetic interactions which arise from the interlayer diffusion process.

For the quadrupolar interaction the transition rates W_1 and W_2 are given by Eqs. (6) and (7) with $I=1$. This type of relaxation would clearly vanish for $\theta=0°$. Thus, we assume that the rate measured at this angle is of magnetic origin and arises from a dipolar coupling between ^{6}Li and ^{7}Li spins. We cannot exclude the presence of some quadrupolar relaxation whose origin is not the interlayer diffusion process. However, this type of quadrupolar relaxation must be exceedingly small since the corresponding EFG fluctuations are much smaller than those arising from the interlayer diffusion process. The dependence of the ^{6}Li relaxation data on temperature and frequency at $\theta=0°$ suggests a BPP-type formula,

$$\frac{1}{T_1}=2W(6)=K^2\frac{\tau}{1+\omega^2\tau^2}\ . \tag{17}$$

With the use of τ values calculated from the parameter set [Eq. (16)] of the ^{7}Li relaxation fit, Eq. (17) yields the theoretical curve for $\theta=0°$ in Fig. 8 with K as the only fitted parameter. Within the error limits a satisfactory agreement is found.

For angles θ different from 0°, both quadrupolar and magnetic interaction can cause the relaxation, and the rate is described by Eq. (5) where the magnetic term is given by Eq. (17) with the additional assumption that it is independent of orientation. Inserting the appropriate values for spin I and coupling constants C_1 and C_2 into the expressions for W_1 and W_2, we obtain

$$\begin{aligned}\frac{1}{T_{1||}(6)}&=W_1(6)+4W_2(6)+2W(6)\\&=\frac{3\pi^2}{4}C^2_{\rm eff}(^6{\rm Li})\left[\sin^2\theta\cos^2\theta\frac{\tau}{1+\tau^2\omega^2}+\sin^4\theta\frac{\tau}{1+4\omega^2\tau^2}\right]+K^2\frac{\tau}{1+\omega^2\tau^2}\ ,\end{aligned} \tag{18}$$

where

$$C^2_{\rm eff}(6)\equiv C^2_1(6)+2C^2_2(6)=1.81\times10^8$$

in units of Hz^2, and the symbol $||$ points to the interlayer process.

Together with the above-mentioned parameter set of Eq. (16) and the parameter K, Eq. (18) was used to evaluate the theoretical curve for $\theta=90°$ in Fig. 8. Again there is good agreement with the experimental data.

Finally, Eq. (18) may be used to fit the angle dependence of the ^{6}Li relaxation rate that we have measured previously[7] at 428 and 535 K (Fig. 9). The fitted parameters were the same as mentioned above. The agreement with the experimental points is satisfying; deviations are attributed to a small angular dependence of the magnetic contribution. In conclusion, all three sets of ^{6}Li relaxation data are consistent with our assumption that the interlayer diffusion is the time-dependent mechanism causing relaxation at higher temperatures.

B. Intralayer diffusion

As stated in Sec. II, the relaxation rates of both Li isotopes at lower temperatures, i.e., around 300 K, are attributed to an intralayer diffusion process. However, in contrast to the relaxation arising from the interlayer diffusion process, no maximum of the relaxation rate is observed. Nevertheless, the angle dependence of the relaxation rates at 300 K provides sufficient information to confirm the presence of the intralayer diffusion process which was found to be responsible for the motional narrowing of the linewidth[11] and to distinguish between different interactions which are responsible for ^{6}Li and ^{7}Li relaxation, respectively.

We start with the ^{7}Li relaxation, which is assumed to be of quadrupolar origin (see Sec. IV). Since only a single relaxation rate is observed, a common spin temperature exists brought about by lattice-induced spin exchange processes.[12] Thus, the relaxation rate is given by Eq. (12). The EFG at a Li site fluctuates whenever a vacancy hops. Therefore we identify $1/\tau_Q$ with the hopping rate of the Li(2) vacancies. Our previously measured data[6] (Fig. 7) may be fitted with any value of τ_Q which satisfies the condition $\omega\tau_Q\leq1$. With $\omega/2\pi=8$ MHz, this means $\tau_Q\leq2\times10^{-8}$ s.

As a by-product of this fit we may estimate the number of Li(2) vacancies, n, i.e., a vacancy concentration c^* which is of the same order of magnitude as the concentration c of Li(1) and Li(2) vacancies we have introduced in Eq. (14). We may estimate c^* in two different ways. One way is to relate τ_Q to

the mean residence time $\bar{\tau}$ of the diffusing ^{7}Li ions by the equation $1/\bar{\tau}=c^*1/\tau_Q$, which is similar to Eq. (14). $\bar{\tau}$ itself is deduced from an analysis of the linewidth data.[11] Around 300 K the line is motionally narrowed and a value of $\bar{\tau}$ ranging from 10^{-7} to 10^{-6} s is obtained, depending on the concentration of hydrogen-nitrogen defects present in the sample. Then, Eq. (12) with the upper limit of τ_Q, i.e., 2×10^{-8} s, yields a concentration c^* of Li(2) vacancies ranging from 0.01 to 0.1. If a shorter τ_Q is used, the range of c^* values shifts to lower concentrations and thus covers even better the x-ray value[16] of $c^*=0.01$.

The second way to obtain the vacancy concentration is to calculate the ratio n/d^4 from Eq. (12). The multiplication factor β is given by[22] $(1+\gamma)(2\epsilon+3)/5\epsilon$, where $\gamma=-0.256$ is the antishielding factor of Li^+ and ϵ the dielectric constant of Li_3N at room temperature[24] with $\epsilon_{\|c}=6$ and $\epsilon_{\perp c}=10.5$. This yields an average value of $\beta=0.356$. With $Q(^7\text{Li})=0.043\times10^{-24}$ cm^2, the upper limit of τ_Q, and $1/T_{1\perp}(7)=5.5$ s^{-1} at $\theta=40°$, Eq. (12) gives

$$n/d^4=6.2\times10^{44},$$

in units of cm^{-6}, or

$$c^*/d^4=3.6\times10^{29},$$

in units of cm^{-4}. Choosing d as the Li(2)-Li(2) distance (2.106 Å), we obtain $c^*=0.07$, which is larger than the x-ray value. If a shorter τ_Q is used, c^* shifts to even larger values. So, in contrast to the first estimate, shorter τ_Q's produce poorer agreement with the x-ray value of c^*.

In the case where we value both estimates equally, then the upper limit of $\tau_Q=2\times10^{-8}$ s represents the best choice, and one obtains a vacancy concentration c^* in the range between 0.01 and 0.1. In view of the simplicity of our diffusion model, the agreement with the x-ray value appears to be fair. Of course, in the second estimate agreement with $c^*=0.01$ could be achieved if we take $d=1.3$ Å. Considering this smaller d, one could speculate that this result points to the fact that Li(2) ions vibrate with larger amplitudes in the direction of neighboring occupied Li(2) sites as found in x-ray studies.[16]

We now turn to the ^{6}Li relaxation data. If the ^{6}Li spin system would also relax by quadrupolar interaction the corresponding rate would be 2000 times smaller than the ^{7}Li rate if the difference in quadrupole moment and radio frequency is considered. The rate measured is only smaller by a factor of about 40. Therefore, the different dependence of the ^{6}Li and ^{7}Li relaxation rates on angular orientation can only be accounted for by assuming quadrupolar relaxation for ^{7}Li and magnetic relaxation for ^{6}Li. With the use of Eq. (13) to describe the angular dependence of the ^{6}Li relaxation rate, the experimental data (see Fig. 9) may be fitted with $\omega_D\tau_D$ values between 0.5 to 1.0; $\omega_D\tau_D=0.8$ appears to be the best fit. With $\omega/2\pi=13.2$ MHz we obtain $\tau_D=0.96\times10^{-8}$ s.

It is surprising that this result comes close to the upper limit for τ_Q. Since the interpretation of τ_D in terms of the vacancy mean jump time is not as straightforward as for τ_Q, it is not clear whether this agreement is accidental or not. To clarify this point before drawing further conclusions another independent determination of τ_Q is necessary. On the other side, one would expect τ_D to be close to $\bar{\tau}$. We believe that the observed discrepancy can partly be attributed to the crudeness of the models used for both the line narrowing and the intralayer diffusion.

C. Comparison with jump rates obtained from conductivity

With the use of the Nernst-Einstein relation, the ionic conductivity at temperature T may be written quite general as

$$\sigma=\frac{nq^2D}{kT},$$

with n the number density of ionic carriers, q their charge, and D their diffusion coefficient. Assuming simple, uncorrelated hopping with τ as the average time for an ion to hop an average distance l, D may be expressed as

$$D=\frac{l^2}{2d\tau},$$

where d is the space dimensionality. Thus we obtain

$$\sigma=\frac{nq^2l^2}{2dkT\tau}. \tag{19}$$

The difference between the mean jump time τ and the correlation time τ_{NMR} inferred from NMR data is taken into account by writing

$$\tau_{\text{NMR}}^{-1}=f\tau^{-1},$$

where f is a correlation factor. f can only be determined if the microscopic details of the diffusion process are known. However, f is always of the order of 1 and therefore may be omitted. Hence, the mean jump time τ may be calculated from Eq. (19)

using the experimental conductivity data.[25] In Fig. 10 are plotted as a function of inverse temperature the $1/\tau$ values obtained from the conductivity parallel to the c axis and the NMR $1/\tau$ values deduced from the interlayer process. The agreement between the three sets of NMR data and the conductivity data is good, thus proving that the Li(1)-Li(2)-Li(1) jump process causes the conductivity parallel to the c axis.

A more refined interpretation taking into account the correlation effects by the so-called Haven ratio[11] is very sensitive to small differences from sample to sample and can only be applied if NMR and conductivity data are taken in the same sample.

VI. SUMMARY

In Li_3N the spin-lattice relaxation times T_1 of ^6Li and ^7Li and the second-order quadrupolar shift of the ^7Li central line were measured as a function of temperature and frequency. The data were analyzed in terms of two different diffusion processes: an interlayer process parallel to the c axis involving Li(1) and Li(2) sites, and an intralayer process perpendicular to the first one and taking place in the Li_2N layer thus involving Li(2) sites only.

In the interlayer process Li ions jump between sites (1) and (2), and the nuclei experience rapidly fluctuating electric and magnetic fields. This diffusion process explains quantitatively three sets of experimental data. First, the temperature and angle dependence of the ^7Li quadrupolar shift is well accounted for, especially the decrease of the shift by a factor of about 100 upon raising the temperature from 400 to 600 K. The activation energy deduced from this analysis is 0.68 ± 0.08 eV.

The second and third set of data are the T_1 values of both Li isotopes measured above 420 K. The strong angle dependence of the relaxation times of ^7Li and ^6Li at various temperatures is explained by assuming quadrupolar relaxation for ^7Li and a mixture of dipolar and quadrupolar relaxation for ^6Li. The analysis of the ^7Li data yields the formation enthalpy 0.2 ± 0.05 eV and the migration energy 0.62 ± 0.3 eV of the Li(2) vacancies. The last value agrees fairly well with the result from the shift measurements and with the value deduced from conductivity.

The same set of parameters which was used to fit the ^7Li relaxation data allowed also a satisfying fit of the ^6Li relaxation time. Thus we have shown that the three sets of experimental data can be interpreted in a consistent manner. Furthermore, the analysis provides correlation times which agree with those obtained from conductivity data. We therefore conclude that the interlayer diffusion process which involves both Li sites is essential for the conductivity parallel to the c axis. This result is in contrast to x-ray studies[16] which postulate an exchange of Li(2) ions belonging to different layers without involving Li(1) ions. The latter process cannot be excluded on the basis of our NMR data but it certainly is not the only process responsible for the interlayer conductivity.

At temperatures below 300 K, the ^6Li and ^7Li relaxation times are explained by an intralayer diffusion process, i.e., isotropic diffusion of Li(2) vacancies in the Li_2N layers. The ^7Li spin system is relaxed by the interaction between the ^7Li quadrupole moment and the electric field gradient due to the vacancy. The relaxation of the ^6Li spins arises from a dipolar coupling with the diffusing ^7Li ions. This interpretation allows us to explain the different behavior of the angle dependence of the ^6Li and ^7Li relaxation times and to estimate the Li(2) vacancy concentration, which agrees fairly well with the x-ray result. In addition, some evidence for the large thermal vibration anisotropy of the Li(2) ions was found.

ACKNOWLEDGMENTS

We wish to thank the Max-Planck-Institut für Festkörperforschung, Stuttgart, for supplying the single crystals. This work was supported in part by the Swiss National Science Foundation. Two of us (R. M. and H. B.) gratefully acknowledge the engagement of Professor A. Seeger in this work.

APPENIX A: CALCULATION OF W_1 AND W_2

Within the framework of first-order perturbation theory, the transition probabilities W_1 and W_2 appearing in Eq. (4) and (5) are related to the upward transition probabilities by[26]

$$W_{m\to m-1}=W_1\frac{(2m-1)^2(I-m+1)(I+m)}{2I(2I-1)^2},$$

$$W_{m\to m-2}=W_2\frac{(I+m-1)(I-m+1)(I+m)}{2I(2I-1)^2},$$

$$W_{m\to m-1}=W(I-m+1)(I+m).$$

W_1 and W_2 themselves are the Fourier transforms of the correlation function of the fluc-

tuating EFG:

$$W_1=\frac{e^2Q^2}{8\hbar^2I}\int_{-\infty}^{+\infty}\langle V_{+1}(t)V_{-1}(0)\rangle \times\exp(-i\omega_{m-1,m}t)dt\ , \tag{A1}$$

$$W_2=\frac{e^2Q^2}{8\hbar^2I}\int_{-\infty}^{+\infty}\langle V_{+2}(t)V_{-2}(0)\rangle \times\exp(-i\omega_{m-2,m}t)dt\ . \tag{A2}$$

Here $\langle\ \rangle$ signifies an ensemble average and $\omega_{m-1,m}$ and $\omega_{m-2,m}$ are the frequencies for the corresponding transitions. $V_{\pm1}$ and $V_{\pm2}$ stand for the following abbreviations:

$$\begin{aligned}V_{\pm1}&=V_{xz}\pm iV_{yz}\ ,\\ V_{\pm2}&=\tfrac{1}{2}(V_{xx}-V_{yy})\pm iV_{xy}\ ,\end{aligned} \tag{A3}$$

where the V_{ij} $(i,j=x,y,z)$ are the components of the EFG tensor in a frame with the polar axis z, parallel to the external magnetic field. With the use of Eq. (A3), we obtain

$$\langle V_{\pm1}(t)V_{-1}(0)\rangle=\langle V_{xz}(t)V_{xz}(0)\rangle\times\langle V_{yz}(t)V_{yz}(0)\rangle\ , \tag{A4}$$

$$\langle V_{+2}(t)V_{-2}(0)\rangle=\tfrac{1}{4}\langle[V_{xx}(t)-V_{yy}(t)]\times[V_{xx}(0)-V_{yy}(0)]\rangle+\langle V_{xy}(t)V_{xy}(0)\rangle\ .$$

The V_{ij}'s may be transformed into the principal axis system x',y',z', where z' is parallel to the symmetry axis of the EFG tensor, and x' and y' are arbitrary since the tensor is axially symmetric. The transformation equations are thus

$$\begin{aligned}V_{xx}-V_{yy}&=\tfrac{3}{2}V_{z'z'}\sin^2\theta\ ,\\ V_{xz}&=\tfrac{3}{2}V_{z'z'}\sin\theta\cos\theta\ ,\\ V_{xy}&=V_{yz}=0\ ,\end{aligned} \tag{A5}$$

and Eq. (A4) becomes

$$\begin{aligned}\langle V_{+1}(t)V_{-1}(0)\rangle&=\tfrac{9}{4}\sin^2\theta\cos^2\theta\langle V_{z'z'}(t)V_{z'z'}(0)\rangle\ ,\\ \langle V_{+2}(t)V_{-2}(0)\rangle&=\tfrac{9}{16}\sin^4\theta\langle V_{z'z'}(t)V_{z'z'}(0)\rangle\ .\end{aligned} \tag{A6}$$

We assume an exponential decay of the correlation function:

$$\langle V_{+1,+2}(t)V_{-1,-2}(0)\rangle=\langle V_{+1,+2}(0)V_{-1,-2}(0)\rangle\exp(-t/\tau)\ ,$$

where the correlation time τ is identified with the mean residence time of an Li atom at a regular lattice site. Then, with the help of Eq. (2) and the definition of the coupling constants,

$$C_k=(eQV_{z'z'}/h)_k \tag{A7}$$

for the sites $k=1,2$, Eq. (A6) yields

$$\left[\frac{eQ}{h}\right]^2\langle V_{+1}(0)V_{-1}(0)\rangle=\tfrac{3}{4}\sin^2\theta\cos^2\theta(C_1^2+2C_2^2)\ ,$$

$$\left[\frac{eQ}{h}\right]^2\langle V_{+2}(0)V_{-2}(0)\rangle=\tfrac{3}{16}\sin^4\theta(C_1^2+2C_2^2)\ .$$

Inserting this into Eqs. (A1) and (A2) we obtain the final result:

$$W_1=\frac{3\pi^2}{4I}(C_1^2+2C_2^2)\sin^2\theta\cos^2\theta\frac{\tau}{1+\omega^2\tau^2}\ , \tag{A8}$$

$$W_2=\frac{3\pi^2}{16I}(C_1^2+2C_2^2)\sin^4\theta\frac{\tau}{1+4\omega^2\tau^2}\ . \tag{A9}$$

We note that $W_1=W_2=0$ for $\theta=0°$ and $W_1=W_2$ for the angle θ^* given by

$$\tan\theta^*=\left[4\frac{1+4\tau^2\omega^2}{1+\tau^2\omega^2}\right]^{1/2}\ . \tag{A10}$$

APPENDIX B: CALCULATION OF $\langle\omega_{\pm1/2}^{(2)}\rangle$

The quadrupolar interaction Hamiltonian is written in the usual form[19]

$$H_Q=\sum_{l=-2}^{+2}Q_lF_l\ ,$$

where the Q_l are quadrupolar operators and the F_l are lattice operators related to the components V_{ij} of the EFG tensor introduced in Eq. (A3) via

$$\begin{aligned}F_0&=V_{zz}=V_0\ ,\\ F_{\pm1}&=\tfrac{1}{3}(V_{xz}\pm iV_{yz})=\tfrac{1}{3}V_{\pm1}\ ,\\ F_{\pm2}&=\tfrac{1}{3}[\tfrac{1}{2}(V_{xx}-V_{yy})\pm iV_{xy}]=\tfrac{1}{3}V_{\pm2}\ .\end{aligned}$$

If the V_l fluctuate according to

$$V_l(t)=\langle V_l\rangle+\delta V_l(t)$$

about their average values $\langle V_l\rangle$ the second-order frequency shifts $\omega_m^{(2)}$ of a nuclear transition will fluctuate as well. Assuming a stationary correlation function for the δV_l, the ensemble average of the second-order frequency shift may be written as [20]

$$\langle\omega_m^{(2)}\rangle=\sum_{l=1}^{2}(\langle m+1\,|\,K_l\,|\,m+1\rangle-\langle m\,|\,K_l\,|\,m\rangle)\times\left[\frac{\langle V_l\rangle\langle V_{-l}\rangle}{l\omega}+\int_0^\infty dt\langle\delta V_l(t)\delta V_{-l}(0)\rangle\sin l\omega t\right], \tag{B1}$$

where

$$K_1=\frac{2}{9}\left[\frac{3eQ}{4I(2I-1)\hbar}\right]^2 I_z[8I_z^2-4I(I+1)+1]\,,$$

$$K_2=\frac{4}{9}\left[\frac{3eQ}{4I(2I-1)\hbar}\right]^2 I_z[-2I_z^2+2I(I+1)-1]\,.$$

We assume that the correlation function of the δV fluctuations is of the form

$$\langle\delta V_l(t)\delta V_{-l}(0)\rangle=\langle\delta V_l(0)\delta V_{-l}(0)\rangle\exp(-t/\tau)\,,$$

where τ is again identified with the mean residence time of an Li nucleus at the Li(1) or Li(2) sites. Then, Eq. (B1) leads to the following expression for the second-order shifts:

$$\langle\omega_m^{(2)}\rangle=\sum_{l=1}^{2}(\langle m+1\,|\,K_l\,|\,m+1\rangle-\langle m\,|\,K_l\,|\,m\rangle)\left[\frac{\langle V_l\rangle\langle V_{-l}\rangle}{l\omega}\frac{1}{1+l^2\omega^2\tau^2}+\frac{\langle V_lV_{-l}\rangle}{l\omega}\frac{l^2\omega^2\tau^2}{1+l^2\omega^2\tau^2}\right].$$

In particular, for the second-order shift of the central component of a quadrupolar splitting for half integer I, we obtain

$$\langle\omega_{-1/2}^{(2)}\rangle=\left[\frac{eQ}{4I(2I-1)\hbar}\right]^2[6-8I(I+1)]\left[\frac{\langle V_{xz}\rangle^2+\langle V_{yz}\rangle^2}{\omega}\frac{1}{1+\omega^2\tau^2}+\frac{\langle V_{xz}\rangle^2+\langle V_{yz}\rangle^2}{\omega}\frac{\omega^2\tau^2}{1+\omega^2\tau^2}\right.$$
$$-\frac{\frac{1}{4}(\langle V_{xx}\rangle-\langle V_{yy}\rangle)^2+\langle V_{xy}\rangle^2}{2\omega}\frac{1}{1+4\omega^2\tau^2}$$
$$\left.-\frac{\frac{1}{4}\langle(V_{xx}-V_{yy})^2\rangle+\langle V_{xy}{}^2\rangle}{2\omega}\frac{4\omega^2\tau^2}{1+4\omega^2\tau^2}\right].$$

For the interlayer diffusion process, the V_{ij} are again given by Eq. (2) and may again be expressed in terms of $V_{z'z'}$. With these substitutions and with $I=\frac{3}{2}$ we are led to the final result for the second-order frequency shift of the ^{7}Li central signal,

$$\langle\omega_{-1/2}^{(2)}\rangle=-\frac{\pi^2}{6\omega}\left[\sin^2\theta\cos^2\theta(C_1+2C_2)^2\frac{1}{1+\omega^2\tau^2}+3\sin^2\theta\cos^2\theta(C_1^2+2C_2^2)\frac{\omega^2\tau^2}{1+\omega^2\tau^2}\right.$$
$$\left.-\tfrac{1}{8}\sin^4\theta(C_1+2C_2)^2\frac{1}{1+4\omega^2\tau^2}-\tfrac{3}{8}\sin^4\theta(C_1^2+2C_2^2)\frac{4\omega^2\tau^2}{1+4\omega^2\tau^2}\right].$$

[1]U. von Alpen, A. Rabenau, and G. H. Talat, Appl. Phys. Lett. 30, 621 (1977).
[2]A. Rabenau, in *Advances in Solid State Physics* (Vieweg, Braunschweig, 1978), Vol. 18, p. 77.
[3]P. J. Haigh, R. A. Forman, and R. C. Frisch, J. Chem. Phys. 45, 812 (1966).
[4]S. G. Bishop, P. J. Ring, and P. J. Bray, J. Chem. Phys. 45, 1525 (1966).
[5]P. K. Burkert, H. P. Fritz, and G. Stefaniak, Z. Naturforsch. Teil B 25, 1220 (1970).
[6]D. Brinkmann, W. Freudenreich, and J. Roos, Solid State Commun. 28, 233 (1978).
[7]D. Brinkman, M. Mali, and J. Roos, *Proceedings of the International Conference on Fast Ion Transport in Solids* (North-Holland, New York, 1979), p. 483.
[8]D. Brinkmann, M. Mali, and J. Roos, Bull. Magn. Reson. 2, 271 (1981).
[9]D. Brinkmann, M. Mali, J. Roos, and R. Messer, Solid State Ionics 5, 409 (1981).
[10]R. Messer, H. Birli, and K. Differt, J. Phys. (Paris) 41, C6 (1981).
[11]R. Messer, H. Birli, and K. Differt, J. Phys. C 14, 2731 (1981).
[12]L. Schimmele and R. Messer, Bull. Magn. Reson. 2, 142 (1981).
[13]R. Messer and H. Birli, Bull. Magn. Reson. 2, 278 (1981).
[14]P. M. Richards, J. Solid State Chem. 33, 127 (1980).
[15]K. Differt and R. Messer, J. Phys. C 13, 717 (1980).
[16]H. Schulz and K. H. Thiemann, Acta Crystallogr. Sec. A 35, 309 (1979).
[17]E. Schönherr, G. Müller, and E. Winkler, J. Cryst. Growth 43, 469 (1978).
[18]E. R. Andrew and D. P. Tunstall, Proc. Phys. Soc. 78, 1 (1961).
[19]A. Abragam, *The Principles of Nuclear Magnetism* (Clarendon, Oxford, 1961).
[20]J. L. Bjorkstam and M. Villa, Phys. Rev. B 22, 5025 (1980).
[21]L. Schimmele, Ph.D thesis, Universität Stuttgart, Stuttgart, West Germany, 1982 (unpublished).
[22]M. H. Cohen and F. Reif, in *Solid State Physics,* edited by H. Ehrenreich, F. Seitz, and D. Turnbull (Academic, New York, 1957), Vol. 5, p. 321.
[23]L. A. Girifalco, *Statistical Physics of Materials* (Wiley, New York, 1973).
[24]H. R. Chandrasekhar, G. Bhattacharya, R. Migoni, and H. Bilz, Solid State Commun. 22, 681 (1977).
[25]J. Wahl, Solid State Commun. 29, 485 (1979).
[26]K. Yosida and T. Moriya, J. Phys. Soc. Jpn. 11, 33 (1956).